A review on computational modelling of individual device components and interfaces of perovskite solar cells using DFT

Cite as: AIP Conference Proceedings **2162**, 020036 (2019); https://doi.org/10.1063/1.5130246
Published Online: 29 October 2019

K. Deepthi Jayan, and Varkey Sebastian

A Review on Computational Modelling of Individual Device Components and Interfaces of Perovskite Solar Cells Using DFT

K. Deepthi Jayan[1, 2, a)] and Varkey Sebastian[1, b)]

[1]*Nirmalagiri College, Kannur University, Kannur, Kerala, 670701, India*
[2]*Rajagiri School of Engineering & Technology, Rajagiri Valley, Kakkanad, Kochi, Kerala, 682039, India*

[a)]Corresponding author: deepthijayan12@gmail.com
[b)]vseba@yahoo.co.in

Abstract. Perovskite structures with the same crystal structure as $CaTiO_3$, are of importance in the field of Materials Science right from the discovery of ceramic high-temperature superconductors to the organic–inorganic semiconductors for high-efficiency photovoltaics. Owing to their unique crystal structure, perovskites display a variety of interesting properties like ferroelectricity, superconductivity, magnetoresistance, birefringence, piezoelectricity etc. Moreover, the efficiency of perovskite solar cells has increased from 3.1% in 2009 to 22.1% in 2017. Since a large number of elements can be combined to form perovskite structures, one can selectively design and optimize perovskite's physical, optical and electrical characteristics. Through theoretical and computational modelling, it is possible to access the hitherto unknown atomistic properties, opto-electronic properties and operational mechanisms of these materials with high accuracy. This paper aims at explaining some of the potentialities of DFT hybrid functionals to analyze the electronic, structural and optical properties of compounds constituting various layers of a perovskite solar cell with the help of software packages like VASP, Wien 2k. Gaussian 09 etc. This paper also reviews the effect of doping on the electronic properties of various layers of perovskite solar cells including the band gap, visible light absorption, relaxation time of holes and electrons using DFT, which in turn determines the optimum charge separation. The effect of introduction of an Intermediate Band Gap in the perovskite structure using DFT methods based on G_0W_0+SOC approach is also discussed here. A study on the effect of various intrinsic defects present in perovskite structures using DFT calculations with VASP package is also discussed. The relevance of modelling the interfaces of various layers of perovskite solar cells with DFT packages is discussed with the help of selected examples of materials and representative interfaces.

INTRODUCTION

Renewable energy sources like solar, biomass, geothermal, hydroelectric, wind etc., which are generally abundant in availability, have emerged as potential alternative to meet world's energy needs over traditional non- renewable energy sources like fossil fuels. Among these renewable sources, solar energy has several advantages over other forms of energy, due to its low cost, high efficiency, modularity and scalability and little adverse environmental impacts. The everlasting quest for improving the efficiency of solar cells resulted in the invention of various semiconductor heterostructures, thin films and other nanomaterials, which can act as potential candidates for the commercial manufacturing of solar cells. However, a detailed knowledge of the electrical, mechanical and optical properties as well as chemical composition of different materials constituting various isolated layers of solar cells is essential for the design of novel high efficiency solar cells. Density Functional Theory (DFT) has become highly popular in this regard owing to the existence of well-established numerical codes capable of describing the ground state properties of various materials [1].

Though the Local Density Approximation (LDA), based on uniform electron density distribution and the Generalized Gradient Approximation (GGA) based on non-uniform electron density distribution, are two well established methods for estimating the ground state electronic properties of materials, they cannot provide accurate results for excited state DFT calculations [2,3]. On the other hand, Hybrid methods tries to incorporate features from first principle methods such as Hartree Fock methods, with some improved DFT mathematics and computational codes. When dealing with computational chemistry applications, B3LYP hybrid method seems to be more reliable than other hybrid methods of DFT calculation, even though most of the hybrid methods depend

Proceedings of the International Conference on Advanced Materials
AIP Conf. Proc. 2162, 020036-1–020036-9; https://doi.org/10.1063/1.5130246
Published by AIP Publishing. 978-0-7354-1907-0/$30.00

on the materials of interest. Another DFT calculation technique using the hybrid functional HSE06 is good for calculating the band offsets, bandgaps etc., but it was found to have certain disadvantages especially when we deal with direct-indirect crossover as in the case of the alloy, GaAsP [4]. GW approach based on Many Body Perturbation Theory (MBPT) can produce reliable results especially when analyzing the electronic and optical properties of materials and can be used self consistently also [5-9]. When interfaces are present, a Super Lattice Approximation is found to be the most reliable approach as it can provide an estimate of band line up [10]. Time Dependent DFT calculations can be used to calculate the frequency dependent molecular response properties of materials like charge carrier transport and charge diffusion [14]. DFT can also shed light into the concepts of electronegativity, hardness, and chemical reactivity index of materials which are essential for analyzing the stability of various perovskite materials [15].

In addition, the dielectric properties of materials play an important role in determining the photon absorption and can be calculated using Density Functional Perturbation theory [11-13]. For analyzing the optical properties, an analysis of bonding and related properties is required and the multipole moments of the compounds can be predicted with DFT [16]. It is also possible to calculate the complex second-order optical susceptibility dispersion for the principal tensor components and their intra-and inter-band contributions [16]. The theoretical circular dichroism spectra of compounds can be calculated using Time Dependent Density Functional Theory [17]. A DFTP method combined with finite difference techniques and symmetry analysis can provide third order components related to physical properties such as nonlinear electrical susceptibilities, nonlinear elasticity or photo elastic and electro strictive effects [18]. The exciton binding energies and related optoelectronic properties like the ionization potentials, electron affinities and fundamental gaps can be calculated using DFT with different density functionals [19].

Computational Modelling of Dye Sensitized Solar Cells (DSSCs)

Soon after O'Regan and Gratzel published their pioneering work in 1991, extensive research has been carried out on improving the efficiency of solar cells, which resulted in the production of energy from sun with renewable materials such as Dye Sensitized Solar Cells (DSSCs) [21-23]. In recent years, researchers took effort to develop new and efficient sensitizers based on ruthenium complexes, zinc porphyrin, natural dyes and metal-free organic dyes, of which, DSSCs based on the first two compounds have achieved efficiencies well above 11% [24-32].

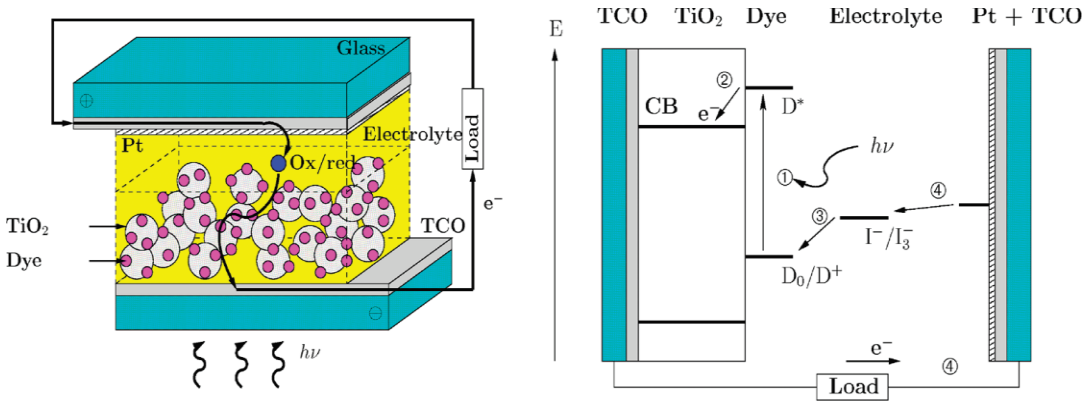

FIGURE 1. DSSC schematic diagram (left) and its working principle (right). Adapted with permission from (F. Labat, P. P. Laine, I. Ciofini and A. Adamo, Chem. Phys. Lett. **417**, 445–451 (2012).) Copyright (2012) American Chemical Society

A detailed description and an accurate prediction of various properties of individual components and interfaces that comprise the fundamental components of Dye Sensitized Solar Cells (DSSCs) can be done with the help of Density Functional Theory (DFT) and Time Dependent Density Functional Theory (TD-DFT) methods [33]. Using a global Hybrid functional (GH) approach such as B3LYP and PBE0 and periodic approach for the treatment and analysis of dye-semiconductor interfaces and semiconductor - electrolyte interfaces with the help of DFT and TD-DFT, Labat et al. showed successfully that it is not only possible to calculate the microscopic properties like the electronic structure and optical properties but also the global parameters like open circuit voltage V_{OC} and the short circuit current density $J_{SC,}$ very accurately [33-36].

Modelling of Isolated Components of DSSCs

Usually a semiconductor material with a conduction band edge well below the excited state of the dye is required for the optimum performance of DSSCs. From the references, it is evident that a DFT study using Global Hybrid Functionals (GH) and Periodic Boundary Conditions (PBCs) can provide a very precise description of the electronic and structural properties of semiconductors, as a component of DSSC assembly [35-38]. However, for the estimation of band gap, a well-developed RSH functional perform better than a GH functional, but for the description of excited state, HSE is not suitable since an exact description of the excited state of both dye and semiconductor is needed for the excited state calculations [33,39].

A component of DSSC, the organic dyes specifically, consist of an electron donating group and an electron withdrawing group in which the excited state, which is responsible for the presence of conduction band electrons of the semiconductor, is generated by the charge transfer from the electron donating group to the electron withdrawing group of the dye. From the references, while taking into consideration the solvent effects, it is evident that the electronic properties of the dye compounds and their absorption spectra can be well described using PBE0 which comes under GH functional approach [40-44].

Modelling of Interfaces of DSSCs

To get high efficiency, the dye molecule must be firmly attached to the semiconductor with the help of various anchoring groups like carboxylic moiety and thus, a modelling of the structural properties of various interfaces of DSSCs becomes very crucial [44]. For the N_3/TiO_2 system, the bi-isonicotinic acid (BINA) molecule as an anchoring group over an anatase (101) surface and for the EY/ ZnO DSSC, a formic acid as an anchoring group over a wurtzite (1010) showed that both anchoring groups react in a dissociative way [37,45]. In a similar way, the structural properties of two anchoring group acetylacetone and catechol for ZnO based applications were analyzed recently and it was found that these groups efficiently anchor the dye to the surface [46,47]. The adsorption geometry obtained from the study of the model systems can next be used to model the real dye/semiconductor interface using PBC.

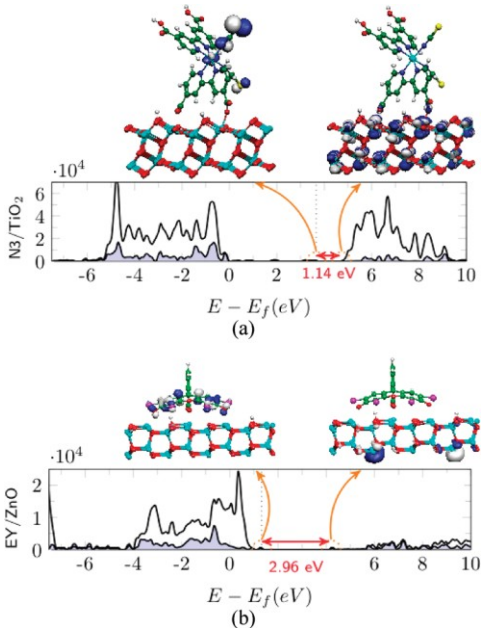

FIGURE 2. Computed densities of states and relevant Γ-point frontier crystalline orbitals of the (a) N_3/TiO_2 (HOMO and LUMO) and (b) EY/ZnO ($HOMOandLUMO^{+2}$) systems.Adapted with permission from (F. Labat, P. P. Lain_e, I. Ciofini and A. Adamo, Chem. Phys. Lett. **417**, 445–451 (2012).) Copyright (2012) American Chemical Society

Finally, an analysis of the structural and electronic properties of the semiconductor-electrolyte interface is to be carried out for the complete modelling of DSSCs. Following the same procedure for the adsorption of the anchoring groups and dyes on the surfaces, Labat et al. investigated the influence of electrolyte composition on the open-circuit voltage (V_{oc}) of DSSC and it was found that a higher V_{oc} can be achieved if the Conduction Band Edge (CBE) energy is higher [48].

Computational Modelling of Perovskite Solar Cells (PSCs)

Other than DSSCs, perovskite structures with the same crystal structure as $CaTiO_3$, are of importance in the field of Materials Science right from the discovery of ceramic high-temperature superconductors to the organic–inorganic semiconductors for high-efficiency photovoltaics. Moreover, the efficiency of perovskite solar cells has increased from 3.1% in 2009 to 22.1% in 2017. There is an ever-increasing quest to develop highly efficient and stable perovskite solar cells and to improve their overall performance. The MAPI- based (Methyl Ammonium Lead Iodide) solar cells have achieved a record Power Conversion Efficiency (PCE) above 22%, which is comparable with single crystalline Si solar cells. However, the stability of these solar cells when exposed to air remains a barrier for its commercialization. One method to improve the stability is to make solid solutions or to mix two or similar elements at the A-site or X-site of perovskite structures [48-50].

The Super Cell (SC) method provides a platform for modelling solid solutions with less computational effort. To reduce the computational cost, the Virtual Crystal Approximation approach (VCA) approach can be employed with pseudopotential plane wave method, where the pseudopotential of virtual atom is constructed by averaging the relevant potentials and wave functions of constituent atoms [51,52]. It has been proved that the VCA approach can provide exact values of lattice constants in cubic phase as a linear function of mixing content, i.e. Vegard's law, for hybrid halide perovskites, though some technical difficulties in calculating the structural and electronic properties are present [53,54]. A non-SCF calculation can be done to obtain the electronic band structure and the density of states (DOS), after performing the structural optimization of supercell. The effective masses of conductive electrons and holes can be obtained by post processing the energy band. Density Functional Perturbation Theory (DFTB) can be used to find out the optical properties like exciton binding energy and absorption coefficient by calculating the frequency-dependent dielectric constants by considering the effect of electron–hole interaction using the Bethe– Salpeter approach [55-58].

As DFT is basically a theory suitable for studying the ground state properties of materials, the standard LDA and GGA approximations usually underestimate the band gap of inorganic perovskites structures. However, for MAPI, PBE or PBEsol approaches, which come under GGA functional, can yield a band gap in agreement with experimental results [59,60]. This arises due to the fact that there exists an error cancellation between the GGA underestimation and the overestimation of calculated band gap due to the lack of Spin Orbit Coupling [61-65], which shows the importance of considering the relativistic effects. This can be done with the help of first-order Scalar Relativistic (SR) and higher order SOC contributions. However, it is necessary to adopt more complex approaches like HSE06, which usually overestimates the band gap of hybrid and all-inorganic perovskites, and hence by combining with SOC treatment, HSE06 can give a reasonable estimation of band gap of inorganic perovskites [66,67]. By combining the GW approximation with the many body interaction studies, it is possible to have an accurate description of electronic structure [68,69].

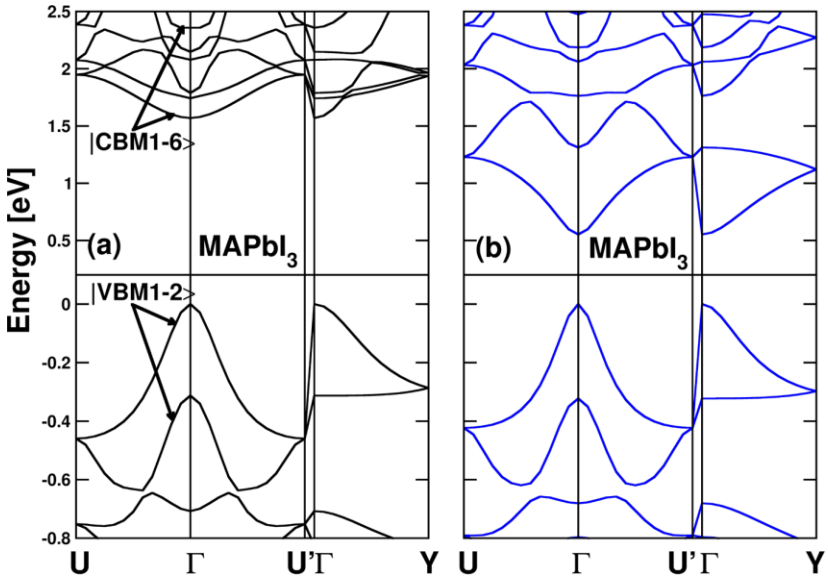

FIGURE 3. Electronic band structure of MAPI (a) without and (b) with spin-orbit interaction. Adapted with permission from (J. Even, L. Pedesseau, J. M. Jancu and C. Katan, J. Phys. Chem. Lett. **4**, 2999–3005 (2013)) Copyright (2013) American Chemical Society

For MAPI, it was found that a small decrease in volume with the action of a small perturbation or a slight increase in pressure results not only in decreasing the band gap in DFT calculations, but also in making a

transition from indirect to direct bandgap. However, the effect of varying the temperature has not yet been studied well for MAPI, even though it was found that a decrease in temperature results in a decrease in band gap [70]. The A site cation has an indirect effect only in the band gap by changing the crystal structure due to the presence of its molecular orbitals far away from the Valence Band Maximum (VBM) whereas substitution on the B-site cation can directly change the conduction band without much change in the crystal structure as a whole. The substitution on the X- site anion can be expected to change the VBM, since the X-site anion dominates the valence bands [71]. Since the conduction electrons and holes combine to form excitons, an analysis of charge carrier transport is important in understanding the performance of the perovskite solar cells and can be done with the help of GW + SOC calculation with the inclusion of a van der Waals (vdW) correction [72,73]. By applying the PBE + SOC approach, Zhao et. al have shown that the electron–acoustic phonon couplings are weak in MAPI, and charge carriers are scattered predominantly by defects or impurities [74]. The paper by K. Lejaeghere et al. contains many references and details of the various computer codes in which 40 different DFT methods were compared to establish high-precision results for equation-of-state data [20].

Modelling of Organohalide Perovskites as ETL

The electronic structure, optical properties and stability of organo-metal halide perovskite structures can be very effectively studied using standard DFT with the help of (PBE) functional [75-77]. However, the estimation of band gap of $MAPbI_3$ using SR DFT gives values in good agreement with experimental results whereas that of $MASnI_3$ shows a variation of 1 eV from the experimental results, approximately [78]. Relativistic effects play a significant role in introducing this band gap differences [77]. However, when Spin Orbit Coupling effects are considered with DFT, there was a band gap underestimation for $MAPbI_3$, which can be resolved by a GW approach incorporating SOC [79,80]. This approach resulted in a SOC-GW absorption spectrum in good agreement with experimental results when electron-hole interactions are neglected [81]. A red shift in wavelength occurs in the absorption spectrum of $MASnI_3$ when compared with $MAPbI_3$, which clearly proves that it is highly suitable for photovoltaic applications [75].

The intermediate band gaps can be introduced into the existing band structure by introducing suitable doping materials and Gregorio Garcia et al. showed that the efficiency of perovskite solar cells can be increased by the partial replacement of Pb with Cr in MAPI perovskite, which leads to the formation of an Intermediate Band Gap (IGB) with the desired properties and hence results in the absorption of two extra photons [82]. However, the band gap calculations with PBEsol+SOC underestimate the experimentally obtained value. Hence G_0W_0+SOC approach, which incorporates spin orbit coupling effects, is implemented to calculate the bandgap of MAPI doped with Cr ions. The band structure analysis shows that the substitution of one Cr atom in place of Pb results in two new energy levels due to the formation of Cr 3d orbital, which can act as IGB.

Defects, surfaces and interfaces play a major role in determining the performance of solar cells. In order to study the effect of such intrinsic defects like Schottky defect or Frenkel defect on the performance of solar cell, an estimation of electronic structures and formation energies is necessary, which were calculated by Jongseob Kim et al. with density functional theory (DFT) using the VASP (Vienna ab initio simulation) program package [83,84]. An expansion of electronic wavefunctions is done with plane waves with a cut off energy of 520 eV and the projector-augmented wave (PAW) method is used to describe the core−valence interaction [85]. The hybrid functional approach with PBE GGA exchange-correlation functional was used and included 5d electrons in the valence charges for Pb. The Monkhorst-Pack sampling with a $4 \times 4 \times 4$ k point grid was selected for obtaining the bulk $CH_3NH_3PbI_3$ structure. The electronic structure was calculated with a $2 \times 2 \times 2$ k-point grid for supercell calculation.

Youveri Wang et al. conducted another study using the VASP package for estimating the structural and electronic properties using the plane-wave projector-augmented wave method [86-90]. A 4×4×4 Monkhorst-pack k-mesh grid was employed for the estimation of structural and electronic properties [91]. For structural relaxation, the van der Waals density functional (vdW-DF) in the form of optB86b-vdW was used which directly provides information about the dispersion interaction between the organic base and the Pb-I framework [92,93]. The electronic properties are studied by using the PBE functional and the modified Becke-Johnson (mBJ) potential by considering the spin-orbit coupling (SOC) effect [94-98]. They investigated the carrier transport and optical properties with the help of band structures obtained from the above-mentioned study. Using deformation potential theory, the optical properties like absorption coefficients and recombination rate were calculated with much denser 20×20×20 k-meshes using the independent particle approximation as implemented in the all-electron WIEN2k code [99,100]. Radi A Jishi et al. reported a DFT based first-principles calculation of six different lead halide semiconductors, namely, $CH_3NH_3PbI_3$, $CH_3NH_3PbBr_3$, $CsPbX_3$ (X=Cl, Br, I), and $RbPbI_3$ using the full potential linear augmented plane wave (LAPW) method with Wien 2k package [100,101]. For these six compounds, excellent agreement was obtained between calculated and experimental band gaps with modified Becke-Johnson exchange and correlation potential. From the study, it was predicted with the help of DFT that the cubic phase of $CsPbI_3$, could be a topological insulator under hydrostatic pressure

[101]. The recent work done by Dongyan Liu et al. clarifies the nature of electronic and mechanical properties of Cs doped $CH_3NH_3PbI_3$, which can be considered as a future candidate for the design of high efficiency and stable hybrid perovskite photovoltaic materials [111-113].

Modelling of Hole Transporters

Hole Transport layer (HTL) plays an important role in photovoltaic energy conversion as the efficiency of a solar cell is highly influenced by the properties of hole transporting materials. Spiro-MeOTAD, (2,2′,7,7′-tetrakis-(N,N-di-4-methoxyphenylamino)-9,9′-spirobifluorene) is found to be the most suitable HTL for perovskite based solar cells, but for DSC, it is Co(II)/Co(III) redox shuttles [102]. One of the main reasons for selecting spiro-MeOTAD as HTL is that its radical cation has two oxidation states, the 2+ and the 4+, and both states exhibit long term stability. An analysis of the excited states of spiro-MeOTAD-derived cations in the absorption processes, when carried out with the help of DFT and TDDFT shows that for the oxidised species maximum absorption of photons occurs in the visible region [103]. As there exists an excellent agreement between theory and experiment while analyzing the electronic, optical and structural properties of both neutral spiro-MeOTAD and its oxidized forms, it can be considered as the most suitable candidate for HTM for both Perovskite Solar Cells and Dye Sensitized Solar Cells. B3LYP exchange-correlation functional can be used to optimize the structure of spiro-MeOTAD and its oxidized forms (spiro-MeOTAD$^+$, spiro-MeOTAD^{2+}, and spiro-MeOTAD^{4+}) in vacuo without taking into consideration any symmetry constraints. Simona Fantacci et al. considered the spin-adapted configurations and DFT calculations like UB3LYP calculations were performed for the mono- and dications of spiroMeOTAD [103].

Modelling of TiO_2 Layer

At finite temperature, Car–Parrinello molecular dynamics plays an important role in sampling the local minima and dynamical fluctuations [106]. As discussed earlier, DFT/TDDFT framework can be used as the most important tool for studying the desired materials and interfacial properties. The cell efficiency, performance, stability and hysteresis of perovskite solar cells are mostly affected by the presence of interfaces. Ali Akbari et al. performed a first principle modelling of perovskite solar cells based on TIO_2 and Al_2O_3 and it was found that the interfacial plane of perovskite significantly influences the energy level alignment between the TiO_2 and perovskite, resulting in the bending of bands for mesoporous perovskite solar cells than that for planar perovskite solar cells [105]. From this study, it was concluded that Al_2O_3 is not suitable for making perovskite solar cells and the addition of Al_2O_3 makes the perovskite solar cells highly unstable.

Modelling of Interfaces and Surfaces

With the help of SOC-DFT calculations, Mosconi and co-workers investigated the interfaces of TiO_2 to MAPI and also $MAPbI_{3-x}Cl_x$ with a small Cl content around 4% [107,108]. The electronic structure calculations using DFT showed that there exists a strong interfacial coupling between the 3d conduction band states of Ti and 6p conduction band states of Pb due to the interaction of perovskite with TiO_2. It was inferred that the same interaction resulted in a slight upliftment of conduction band energy of TiO_2 [109]. It was also found that the presence of defects at interfaces modify the band alignment, thus leading to the bending of perovskite bands close to the TiO_2 surface, which results in the generation of trap states. In order to understand the cases of all-inorganic perovskites, the $CsPbBr_3/TiO_2$ heterostructure has been investigated by Qian et al. using the PBEsol+HSE06 functional [110]. It was found that a large charge transfer occurs between Cs and O atoms due to the presence of interface defects, whereas a less charge transfer between Br and Ti atoms occurs [114].

CONCLUSION

In this review, a critical theoretical analysis based on first principle DFT calculations of the structural properties, electronic and optical properties, lattice dynamics and material stabilities, effect of defects on performance and the influence of surfaces and interfaces in the hybrid organic–inorganic and purely all-inorganic halide perovskites are discussed. Since stability is a major concern for the commercialization of PSCs, the study on degradation of perovskite materials under humid and wet conditions and chemical stability analysis of MAPI are also included here. Though research on band gap tuning, band gap engineering, defect study, search for lead free perovskites etc. have been carried out successfully, the topics like photon percolation into the interface and its influence on the overall performance of PSCs still remain unattended. The doping strategy

has been scarcely explored for Pb-free perovskite systems and further exploration for a precise composition is expected to bring substantial changes in photovoltaic research.

ACKNOWLEDGEMENT

The author acknowledges the faculty members of the Department of Physics, Nirmalagiri College, Kannur University, for their endless support, guidance and encouragement.

REFERENCE

1. J. Even. et. al., International Journal of Photoenergy, 1-11 (2014).
2. J. P. Perdew and Y. Wang, *Physical Review B: Condensed Matter and Materials Physics***98**, 13244-13249 (1992).
3. J. P. Perdew, K. Burke, and M. Ernzerhof, *Physical Review Letters* **77**, 3865–3868 (1996).
4. J. W. Nicklas and J. W. Wilkins, *Applied Physics Letters***97**, 091902 - 091902 (2010)
5. M. P. Surh, S. G. Louie, and M. L. Cohen, *Physical Review B: Condensed Matter and Materials Physics* 43, 9126–9132 (1991).
6. N. Chimot, J. Even, H. Folliot, and S. Loualiche, *Physica B: Condensed Matter***364**, 263–272 (2005).
7. P. Prodhomme, F. Fontaine-Vive, A. V. D. Geest, P. Blaise, and J. Even, *Applied Physics Letters***99**, 022101 (2011).
8. M. van Schilfgaarde, T. Kotani and S. Faleev, *Physical review letters* **96**, 226402 (2006).
9. J. Vidal, F. Trani, F. Bruneval, M. A. L. Marques and S. Botti, Physical Review Letters **104**, 136401 (2010).
10. P. Prodhomme, F. Fontaine-Vive, A. V. D. Geest, P. Blaise, and J. Even, Applied Physics Letters 99, 022101 (2011).
11. S. Baroni, P. Gianozzi, and A. Testa, *Physical Review Letters***59**, 2662 (1987).
12. X. Gonze and J.-P. Vigneron, *Physical Review B: Condensed Matter and Materials Physics***39**, 13120–13128 (1989).
13. X. Gonze, B. Amadon, P.-M. Anglade et al., *Computer Physics Communications***180**, 2582– 2615 (2009).
14. S. J. A. van Gisbergen, V. P. Osinga, O. V. Gritsenko, R. van Leeuwen, J. G. Snijders, and E. J. Baerends, *Journal of Chemical Physics***105,** 3142-3151 (1996).
15. W. Kohn, A. D. Becke and R. G. Parr, *J. Phys. Chem.**100***, 12974–12980 (1996)
16. I. MeradBoudia, A. H. Reshak, T. Ouahrani, and Z. Bentalha, *Journal of Applied Physics* **113**, 083505 (2013)
17. T. Mori, Y. Inoue and S. Grimme, *The Journal of organic chemistry***71**, 9797-9806 (2006).
18. L. Pedesseau, C. Katan, and J. Even, Applied Physics Letters **100**, 031903 (2012).
19. J.C. Lee, J.D. Chai and S.T. Lin. *RSC Advances* ***5***,101370-101376 (2015).
20. K. Lejaeghere, G. Bihlmayer, T. Björkman, P. Blaha, S. Blügel, V. Blum, D. Caliste, I.E. Castelli, S. J. Clark, A. Dal Corso, and S. De Gironcoli, *Science* **351**, aad3000 (2016).
21. B. O'Regan, M. Gratzel, *Nature***353**, 737–740 (1991).
22. A. Hagfeldt, G. Boschloo, L. Sun, L. Kloo, H. Pettersson, *Chem. Rev*. **110**, 6595–6663 (2010).
23. M. T. Spitler and B. A. Parkinson, *Acc. Chem. Res*. **42**, 2017–2029 (2009).
24. M. Gratzel, *Inorg. Chem*. **44**, 6841−6851 (2005).
25. M. Gratzel, *MRS Bull*.**30**, 23−27 (2005).
26. N. Robertson, *Angew. Chem*. **45**, 2338−2345 (2006).
27. C. M. Lan, H. P. Wu, T.Y. Pan, C. W. Chang, W. S. Chao, C. T. Chen, C. L. Wang, C. Y. Lin and E. W. G. Diau, *Energy Environ. Sci*. 2012 **5**, 6460−6464 (2012).
28. X. F. Wang and H. Tamiaki, *Energy Environ. Sci. 2010*, **3**, 94−106 (2010).
29. W. M. Campbell, K.W. Jolley, P. Wagner, K. Wagner, P. J. Walsh, K. C. Gordon, L. Schmidt-Mende, M. K. Nazeeruddin, Q. Wang, M. Gratzel et al., *J. Phys. Chem. C* **111**, 11760−11762 (2007).
30. H. Dong, X. Zhou and C. Jiang, *Theor. Chem. Acc.***131**, 1102 (2012).
31. M. Pastore, F. D. Angelis, *Science***4**, 556−562 (2010).
32. M. Planells, L. Pelleja, J. N. Clifford, M. Pastore, F. De Angelis, N. Lopez, S. R. Marder and E. Palomares, *Energy Environ. Sci.***4**, 1820−1829 (2011).
33. F. Labat, T. Le Bahers, I. Ciofini, and C. Adamo, *Accounts of Chemical Research* **45**, 1268–1277 (2012).
34. M. Marsman, J. Paier, A. Stroppa and G. Kresse, *J. Phys.: Condens. Matter***20**, 064201 (2008).
35. F. Labat, P. Baranek, C. Domain, C. Minot and C. Adamo, *J. Chem. Phys*. **126**, 154703 (2007).
36. L. Labat, Ph. Baranek and C. Adamo, *J. Chem. Theory Comput.***4**, 341– 352 (2008).
37. F. Labat, I. Ciofini and C. Adamo, *J. Chem. Phys.***131**, No. 044708 (2009).

38. F. Cora, M. Alfredsson, G. Mallia, D. S. Middlemiss, W. C. Mackrodt, R. Dovesi and R. Orlando, *Struct. Bonding (Berlin)***113**, 171–232 (2004).
39. J. Heyd, and G. Scuseria, *J. Chem. Phys*. **121**, 1187–1192 (2004).
40. T. Le Bahers, T. Pauport_e, G. Scalmani, C. Adamo and I. Ciofini, *Phys. Chem. Chem. Phys.***11**, 11276–11284 (2009).
41. J. F. Guillemoles, V. Barone, L. Joubert and C. Adamo, C., *J. Phys. Chem. A***106**, 11354–11360 (2002).
42. M. Rekhis, F. Labat, O. Ouamerali, I. Ciofini and C. Adamo, *J. Phys. Chem. A***111**, 13106–13111 (2008).
43. S. Hazebrouck, F. Labat, D. Lincot and C. Adamo, *J. Phys. Chem.* A **112**, 7264–7270 (2008).
44. F. Labat, P. P. Laine, I. Ciofini and A. Adamo, *Chem. Phys. Lett*. **417**, 445–451 (2006).
45. F. Labat and C. Adamo, *J. Phys. Chem. C***111**, 15034–15042 (2007).
46. T. Le Bahers, T. Pauport_e, F. Labat, G. Lef_evre and I. Ciofini, *Langmuir***27**, 3442–3450 (2011).
47. T. Le Bahers, T. Pauport_e, F. Labat, F. Odobel and I. Ciofini, *Int. J. Quantum Chem*. **112**, 2062–2071 (2012).
48. T. Le Bahers, F. Labat, T. Pauport_e and I. Ciofini, *Phys. Chem. Chem. Phys.***12**, 14710–14719 (2010).
49. S. Chatterjee and A. J. J. Mater. *Chem. A***6**, 3793–823 (2018).
50. L.K. Ono, E. J. Juarez-Perez and Y. Qi, *ACS Appl. Mater. Interfaces***9**, 30197–246 (2017).
51. C. J. Yu and H. Emmerich, *J. Phys.: Condens. Matter***19**, 306203 (2007).
52. J. Íniguez, L. Bellaiche and D., *Phys. Rev. B***67**, 224107 (2003).
53. U. G. Jong, C. J. Yu, J. S. Ri, N. H. Kim and G. C. Ri, *Phys. Rev. B***94**, 125139 (2016).
54. U. G. Jon, C. J. Yu, Y. M. Jang, G. C. Ri, S. N. Hong and Y. H. Pae, *J. Power Sources***350**, 65–72 (2017).
55. S. Baroni, S. de Gironcoli, A. Dal Corso and P. Giannozzi, *Rev. Mod. Phys*. **73**, 515–62 (2001).
56. S. Sharma, J. K. Dewhurst and C. Ambrosch-Draxl C, *Phys. Rev. B***67**, 165332 (2003).
57. S. Sharma and C. Ambrosch-Draxl, *Phys. Scr. T***109**, 128 (2004).
58. G. Onida, L. Reining and A. Rubio, 2002, *Rev. Mod. Phys*. **74**, 601–59 (2002).
59. J. P. Perdew, K. Burke and M. Ernzerhof, *Phys. Rev. Lett*. **77**, 3865 (1996).
60. J. P. Perdew, A. Ruzsinszky, G. I. Csonka, O. A. Vydrov, G. E. Scuseria, L. A. Constantin, X. Zhou and K. Burke, *Phys. Rev. Lett*. **100**, 136406 (2008).
61. J. Even, L. Pedesseau and C. Katan, *J. Phys. Chem.C***118**, 11566–72 (2014).
62. J. Even, L. Pedesseau, J. M. Jancu and C. Katan, *J. Phys. Chem. Lett.***4**, 2999–3005 (2013).
63. C. Motta, F. El-Mellouhi, S. Kais, N. Tabet, F. Alharbi and S. Sanvito, *Nat. Commun*. **6**, 7026 (2015).
64. G. Giorgi, J. I. Fujisawa, H. Segawa and K. Yamashita, *J. Phys. Chem. Lett*. **4**, 4213–6 (2013).
65. P. Azarhoosh, S. McKechnie, J. M. Frost, A. Walsh and M. van Schilfgaarde, *APL Mater.***4**, 091501 (2016).
66. J. Heyd, G. E. Scuseria and M. Ernzerhof, *J. Chem. Phys*. **118**, 8207–15 (2003).
67. J. Heyd and G. E. Scuseria, *J. Chem. Phys.***121**, 1187 (2004).
68. F. Brivio, K. T. Butler, A. Walsh and M. van Schilfgaarde, *Phys. Rev. B***89**, 155204 (2014).
69. L. Huang and W. R. L. Lambrecht, *Phys. Rev. B***88**, 165203 (2013).
70. Y. Yamada and T. Nakamura, *Appl. Phys. Express***7**, 032302 (2014).
71. R. Lindblad, N. K. Jena, B. Philippe, J. Oscarsson et al., *J. Phys. Chem.C***119**, 1818–25 (2015).
72. P. Umari, E. Mosconi and F. De Angelis, *Sci. Rep*. **4**, 4467 (2014).
73.]. S. Grimme, J. Comput. Chem. 27 1787–99 (2006).
74. T. Zhao, W. Shi, J. Xi, D. Wang and Z. Shuai, *Sci. Rep*. **7**, 19968 (2016).
75. J. Burschka, N. Pellet, S. M. Moon, R. Humphry-Baker, P. Gao, M. K. Nazeeruddin and M. Grätzel, *Nature* **499**,316– 319 (2013).
76. M. Liu, M. B. Johnston and H. J. Snaith, *Nature* 501, 395– 398 (2013).
77. E. Mosconi, A. Amat, M. K. Nazeeruddin, M. Grätzel and F. De Angelis, *J. Phys. Chem. C* 117, 13902–13913 (2013).
78. I. E. Castelli, T. Olsen, S. Datta, D. D. Landis, S. Dahl, K. S.Thygesen and K. W. Jacobsen, *Energy Environ. Sci.* 5, 5814–5819 (2012).
79. J. Even, L. Pedesseau, J. M. Jancu and C. Katan, *J. Phys. Chem. Lett.* 4, 2999– 3005 (2013).
80. R. Sakuma, C. Friedrich, T. Miyake, S.Blügel and F.Aryasetiawan, *Phys. Rev. B* **84**, 8408514 (2011).
81. P. Umari, E. Mosconi and F. De Angelis, *Sci. Rep.*4, 4467 (2014).
82. G. García, P. Palacios, E. Menéndez-Proupin, A. L. Montero-Alejo, J. C. Conesa and P. Wahnón, *Scientific reports* **8**,.2511 (2018).
83. G. Kresse, J. Hafner, *Phys. Rev. B***47**, 558 (1993).
84. G. Kresse and J. Furthmüller, Comput. Mater. Sci. 6, 15−50 (1996).
85. P. E. Blö chl, *Phys. Rev. B***50**, 17953−17979 (1994).
86. G. Kresse, *Phys. Rev. B***54**, 11169-11186 (1996).
87. G. Kresse and J. Furthmüller, *Comp. Mater. Sci*. **6**, 15-50 (1996).
88. P. E. Blochl, *Phys. Rev. B***50**, 17953-17979 (1994).

89. G. Kresse, *Phys. Rev. B* **59**, 1758-1775 (1999).
90. Y. Wang, Y. Zhang, P. Zhang and W. Zhang, *Physical Chemistry Chemical Physics* **17**, 11516-11520 (2015).
91. H. J. Monkhorst and J. D. Pack, *Phys. Rev .B* **13**, 5188-5192 (1976).
92. M. Dion, H. Rydberg, E. Schroder, D. C. Langreth and B. I. Lundqvist, *Phys. Rev .Lett.* **92**, 246401 (2004).
93. J. Klimes, D. R. Bowler and A. Michaelides, *Phys. Rev. B* **83**, 195131 (2011).
94. J. P. Perdew, K. Burke and M. Ernzerhof, *Phys. Rev. Lett* **77**, 3865-3868 (1996).
95. A. D. Becke and E. R. Johnson, *J. Chem. Phys.* **124**, 221101 (2006).
96. F. Tran and P. Blaha, *Phys. Rev. Lett.* **102**, 226401 (2009).
97. D. Koller, F. Tran and P. Blaha, *Phys. Rev. B* **83**, 195134 (2011).
98. D. Koller, F. Tran and P. Blaha, *Phys. Rev. B* **85**, 155109 (2012).
99. W. Shockley and H. J. Queisser, *J. Appl. Phys*. **32**, 510 (1961).
100. P. Blaha, K. Schwarz, G. Madsen, D. Kvasnicka and J. Luitz, *WIEN2k* (Karlheinz Schwarz, Techn. Universität Wien, Austria, 2001).
101. R. A. Jishi, O. B. Ta and A. A. Sharif, *The Journal of Physical Chemistry C* **118**, 28344-28349 (2014).
102. Z. Hawash, L.K. Ono and Y. Qi, *Advanced Materials Interfaces* **5**, 2018.
103. S. Fantacci, F. De Angelis, M. K. Nazeeruddin and M. Grätzel, M., *The Journal of Physical Chemistry C* **115,** 23126-23133(2011).
104. E. J. Juarez-Perez, M. R. Leyden, S. Wang, L. K. Ono, Z. Hawash and Y. Qi, *Chemistry of Materials* **28**, 5702-5709 (2016).
105. M. Ouafi, B. Jaber, L. Atourki, R. Bekkari and L. Laânab, *Journal of Alloys and Compounds* **746**, .391-398 (2018).
106. F. de Angelis, *Accounts of chemical research* **47**, 3349-3360 (2014).
107. E. Mosconi, E. Ronca and F. de Angelis, *The journal of physical chemistry letters* **5**, 2619-2625 (2014).
108. V. Roiati, E. Mosconi, A. Listorti, S. Colella, G. Gigli and F. de Angelis, **14**, 2168-2174 (2014).
109. E. Mosconi, E. Ronca and F. de Angelis, *The journal of physical chemistry letters* **5**, 2619-2625 (2014).
110. C. X. Qian, Z. Y. Deng, K. Yang, J. Feng, M. Z. Wang, Z. Yang, S. Liu. and H. J. Feng, *Applied Physics Letters* **112**, 093901 (2018).
111. D. Liu, S. Li, F. Bian and X. Meng, *Materials* 11, 1141 (2018).
112. L. Protesescu, S. Yakunin, M.I. Bodnarchuk, F. Krieg, R. Caputo, C. H. Hendon, R. X. Yang, A. Walsh and M.V. Kovalenko,*Nano Lett.* 15, 3692–3696 (2015).
113. G. Murugadoss and R. Thangamuthu, *Solar Energy*, 179, 151-163 (2019).
114. L. K. Ono, E. J. Juarez-Perez, and Y. Qi, *ACS applied materials & interfaces*, 9, 30197-30246 (2017).